DOI: 10.1002/ejoc.200801211

Controlling Selectivity for Cycloadditions of Nitrones and Alkenes Tethered by Benzimidazoles: Combining Experiment and Theory

Liping Meng,[a] Selina C. Wang,[a] James C. Fettinger,[a] Mark J. Kurth,*[a] and Dean J. Tantillo*[a]

Keywords: Nitrones / Cycloaddition / Quantum chemical calculations / Stereoselectivity / Substituent effects / Transition states

Herein we describe a combined experimental/theoretical study on the effects of substituents on regio- and stereoselectivity in intramolecular 1,3-dipolar cycloadditions of nitrones and alkenes tethered by benzimidazoles. By employing a large substituent at position R^2 or R^3, complete selectivity was achieved for either the fused or bridged cycloadduct, respectively. In addition, these cycloadducts were formed as single diastereomers in all of the cycloadditions examined.

Introduction

Dipolar cycloadditions play a central role in modern heterocycle synthesis.[1] Many variations in both the dipole and dipolarophile cycloaddition partners have been explored, as have inter- and intramolecular reaction manifolds, and the effects of various promoters. Although nitrone-alkene cycloaddition reactions have been utilized in the synthesis of many isoxaolidines, including those which form the cores of potential antifungal and antibacterial agents (e.g., **1**),[2,3] some aspects of this chemistry would benefit from more detailed understanding. Herein we describe a combined experimental/theoretical study on the family of intramolecular nitrone-alkene cycloadditions shown in Scheme 1.[4] This study originated from a synthetic project aimed at constructing libraries of conformationally constrained[5] isoxazolidines with potential biological activity.[6] Quantum chemical calculations were employed to help rationalize the regio- and stereoselectivity observed in these initial experiments. The success of this approach then led to computation-based predictions of product distributions for additional reactions, which were put to the test experimentally. Ultimately, a synergistic back-and-forth between synthetic and theoretical chemistry, with each suggesting new experiments for the other, led to a complete picture of the reactivity for the systems shown in Scheme 1.

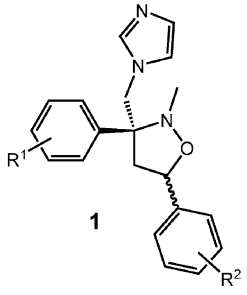

1

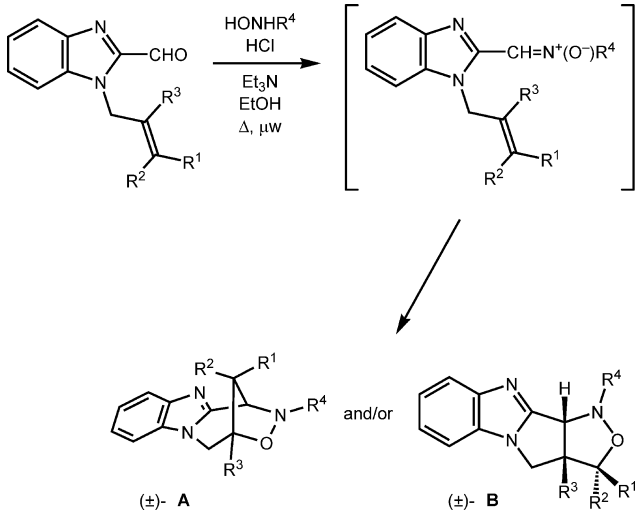

Scheme 1.

Results and Discussion

Overview

Experimentally determined product distributions and computed relative energies of transition-state structures leading to each product (see Exp. Sect. for computational

[a] Department of Chemistry, University of California, Davis, One Shields Avenue, Davis, CA 95616, USA
E-mail: djtantillo@ucdavis.edu
mjkurth@ucdavis.edu

Supporting information for this article is available on the WWW under http://www.eurjoc.org or from the author.

Table 1. Summary of experimental yields[a] and computed transition-state energies[b] for systems with a variety of substitution patterns.[c]

Entry	R^1	R^2	R^3	R^4	% Yield of **A**	% Yield of **B**	TS for **A** [kcal/mol]	TS for **B** [kcal/mol]
1	H	H	H	Me	**63**	25	**20.3**	22.5
2	H	H	H	*i*Pr	**61**	37	–	–
3	H	H	H	*t*Bu	**69**	28	–	–
4	H	H	H	*c*Hex	**79**	19	**22.8**	26.4
5	H	H	H	Bn	**64**	31	–	–
6	H	H	H	Ph	**64**	21	**17.8**	19.2
7	Me	H	H	*c*Hex	**49**	31	**25.8**	**25.8**
8	Ph	H	H	*c*Hex	17	**69**	**24.0**	25.2
9	*t*Bu	H	H	*c*Hex	0	0	30.0	**26.5**
10	*t*Bu	H	H	Me	0	**44**	28.3	**23.8**
11	H	*t*Bu	H	*c*Hex	0	**96**	30.7	**24.2**
12	H	*t*Bu	H	Me	0	**97**	23.5	**19.3**
13	Me	Me	H	*c*Hex	9	**85**	31.5	**27.8**
14	Me	Me	H	Ph	3	**97**	23.5	**19.3**
15	H	H	Me	*c*Hex	**98**	0	**23.1**	28.3
16	H	H	Me	Me	**96**	0	**21.2**	25.5
17	H	H	*t*Bu	*c*Hex	**97**	0	**22.4**	29.7
18	H	H	Ph	*c*Hex	**96**	0	**21.6**	27.0
19	H	H	Ph	Me	**96**	0	**21.3**	25.7

[a] The yields are isolated yields from experiments carried out in ethanol with microwave irradiation at 80 °C for 30 min.[7] [b] B3LYP/6-31G(d); energies are relative to the lowest energy nitrone conformer found for each system (i.e., various conformations of the nitrone- and alkene-containing chains were examined).[7] [c] Bold values correspond to the major product observed experimentally or predicted theoretically.

methods) are shown in Table 1 for the simplest systems studied experimentally.[7] Although mixtures of products **A** and **B** were sometimes observed, these products were formed as single diastereomers. For nearly all cases (all but Entries 7 and 8), the transition-state structure with the lower computed energy corresponds to the experimentally observed major product.[8] For Entry 7, no selectivity is predicted computationally, but a slight selectivity is observed experimentally. For Entry 8, a preference for product **A** is predicted computationally, but a preference for **B** is observed experimentally. Note that these two cases are the two cases for which the computed transition-state-structure energies are closest to each other; this shows the limits of our computational approach. Note also that our calculations were not biased by knowledge of the experimental results; in fact, in some cases, the computational prediction preceded the experiment. Overall, the agreement between theory and experiment is excellent. The sections that follow highlight various aspects of the chemistry that is summarized in Table 1.

Closely related dipolar cycloadditions have been described previously.[4] Of particular note is the seminal work of Zecchi, Beccalli, Broggini, and co-workers. These authors examined systems with imidazole (R^1 = R^2 = R^3 = H, R^4 = Bn or phenylethyl),[4a] pyrrole or butylpyrrole (R^1 = H, Me, Pr, Ph, R^2 = H, Me, R^3 = H, R^4 = Bn, phenylethyl),[4b] and indole (R^1 = Ph, R^2 = H, R^3 = H, R^4 = H, Bn, phenylethyl) tethers.[4c] Our results on systems with substitution patterns similar to these further suggest that the heterocycle used as a tether does not significantly influence the selectivity of the cycloaddition reactions. Our experiments and quantum chemical calculations involve systems with a variety of additional substitution patterns – systems that were explored in a systematic attempt to clarify the importance of the substituents R^1–R^4 in controlling the **A** vs. **B** selectivity. These experiments show that either of the polycyclic scaffolds found in products **A** and **B** can be obtained to the exclusion of the other if substituents are chosen judiciously.

Synthesis of Reactants

The requisite 1-substituted allyl-1*H*-benzo[*d*]imidazole-2-carbaldehydes (nitrone precursors) were prepared from *o*-diaminobenzene in analogy to our previous work[6] as shown in Scheme 2. Commercially unavailable allylic bromides or mesylates were prepared according to reported methods.[9–17] It is worth mentioning that decarbonylation[18] was observed in some cases during conversion of the acetal to the aldehyde. This side reaction could be

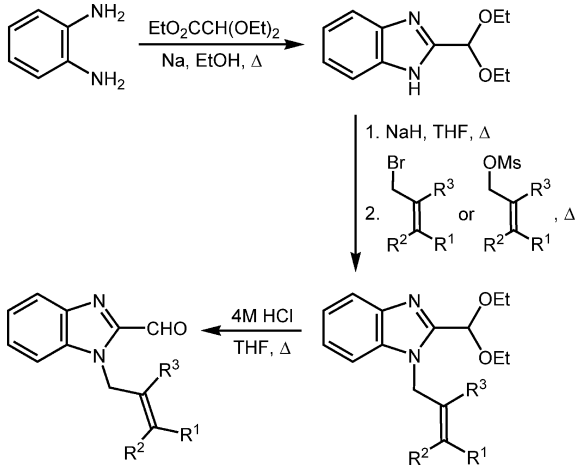

Scheme 2.

suppressed to some extent by using more dilute HCl. Details on the specific conditions used and yields for these reactions can be found in the Supporting Information.

Cycloaddition Reactions

The intramolecular cycloadditions discussed herein (Scheme 1 and Table 1) were carried out in ethanol with microwave irradiation at 80 °C for 30 min, unless otherwise noted. Note that nitrones were generated in situ by the condensation of a given hydroxylamine ($HONHR^4$) with the carbaldehyde reactant. Preliminary experiments utilized conventional heating (as was done in most previous studies on closely related systems[4a–4c]; our systems were refluxed in ethanol for 24 h; see Supporting Information for details), but using microwave irradiation reduced the reaction times while leading to similar yields.[4d] No significant changes in selectivity were observed between the conventionally heated and microwave-irradiated reactions. All products were thoroughly characterized by NMR and some product assignments were corroborated by X-ray diffractometric analysis (Figure 1) and/or chemical shift assignments derived from quantum chemical calculations (see Supporting Information).

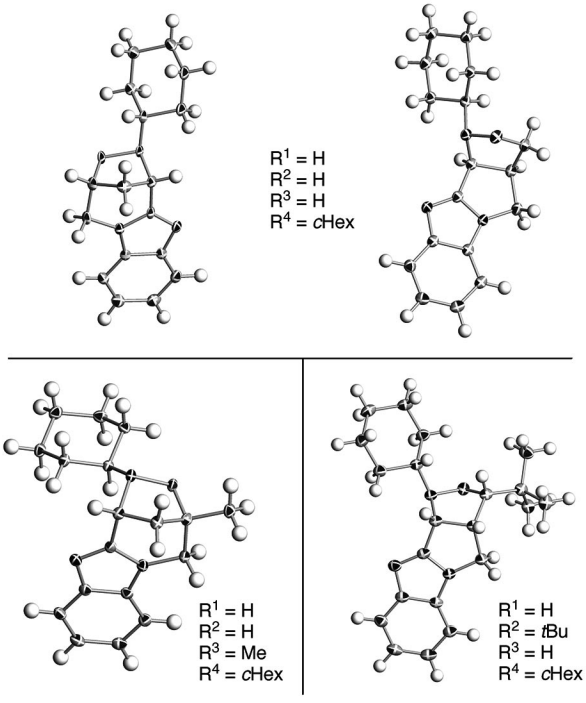

Figure 1. X-ray structures of several cycloadducts (see Table 1, Entries 4, 11, and 15).

Connecting Nitrone and Product Structures

For the cycloadditions described above, nitrones were generated in situ. Consistent with this assumption, when the alkyne (rather than alkene) substituted system shown in Figure 2 was subjected to the reaction conditions, cycloaddition did not occur, but a nitrone was isolated and its structure verified by X-ray crystallography (Figure 2).[4c,19] Additional heating at a higher temperature (120 °C, EtOH, μW, 45 min) led to the rearrangement of the nitrone functional group to an amide (and to a lesser amount of an ester; Figure 2).[20,21] Moreover, when the R^1 = *t*Bu, R^2 = R^3 = H, R^4 = *c*Hex system (Table 1, Entry 9) was subjected to the usual reaction conditions, no cycloadducts were isolated (the importance of the R^1 and R^4 substituents are discussed below). NMR spectroscopic data (see Supporting Information) suggested that a nitrone was formed but again did not react further, and additional heating at a higher temperature again led to an amide product (the same is true for the terminal alkyne analogue of the system shown in Figure 2; see Supporting Information). Similarly, the R^1 = *t*Bu, R^2 = R^3 = H, R^4 = Me system (Table 1, Entry 10) also led to a mixture of nitrone isomers (54%) in addition to product **B** (see Supporting Information).

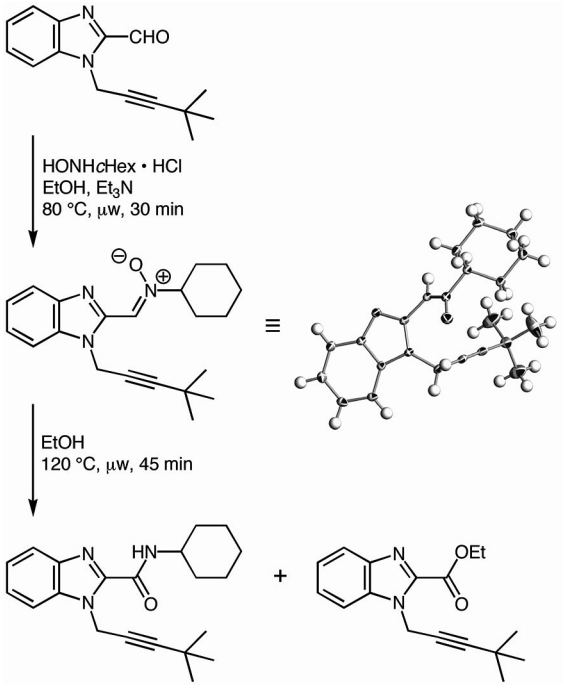

Figure 2. Attempted cycloaddition of an alkyne-substituted reactant and X-ray structure of the nitrone product isolated.

Our calculations suggest that the stereochemistry of a given nitrone (*E* or *Z*) is directly translated into which type of cycloaddition (formation of product **A** or **B**) occurs. In short, for geometric reasons, a (*Z*)-nitrone leads directly to the transition-state structure for formation of product **A**, while an (*E*)-nitrone leads directly to the transition-state structure for formation of product **B** (in the specific benzimidazole-tethered systems we describe herein); i.e., no transition-state structures with different relative orientations of the dipole and alkene (*endo*/*exo*) were located. Representative transition-state structures for the formation of products **A** and **B** are shown in Figure 3 (for the R^1 = R^2 = R^3 = H, R^4 = Me system). The (*E*) or (*Z*) stereochemistry of the nitrone precursors is apparent in these transition-state structures. For no case was a transition-state structure

for formation of product **A** found with an (*E*)-like nitrone substructure, nor was any transition-state structure for formation of product **B** found with a (*Z*)-like nitrone substructure.

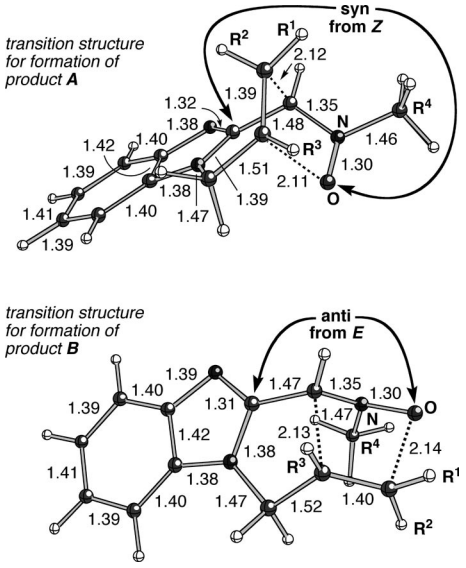

Figure 3. Computed [B3LYP/6-31G(d)] transition-state structures for cycloadditions leading to products **A** and **B** with $R^1 = R^2 = R^3 = H$, $R^4 = Me$. Selected distances are shown in Å.

The direct translation of nitrone stereochemistry into product structure, coupled with the strong correspondence between experimentally observed selectivity and predicted relative energies of transition-state structures[22] (vide supra) suggests that the cycloaddition reactions occur under Curtin–Hammett conditions,[23] i.e. the nitrone precursors interconvert rapidly under the reaction conditions, allowing the product distributions to reflect the relative energies of the competing transition-state structures. What is the mechanism by which nitrone isomerization takes place? Our calculations on a small model system (Scheme 3) suggest that simple rotation about the C=N bond (we were unable to locate any transition-state structure for such a process) or formation of a diradical or oxaziridine intermediate under thermal conditions (barriers for each of >50 kcal/mol) are unlikely (photochemical generation of such species cannot be definitively ruled out for our reaction conditions).[20,21,24] Scheme 4 shows an experiment that suggests another possible pathway for isomerization. A nitrone with R^4 = Me but not bearing an alkene was synthesized (*Z*:*E*, 3:1 in [D_6]-DMSO; *Z*:*E*, 1.1:1 in [D_6]benzene)[25a] and subjected to the usual reaction conditions for cycloaddition in the presence of a hydroxylamine with a different R^4 group (*c*Hex). Under these conditions, the nitrone bearing the *c*Hex group was formed in 80% yield as the (*Z*)-nitrone,[25b] suggesting

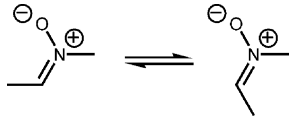

Scheme 3.

that hydroxylamine exchange can occur under our reaction conditions (e.g., excess hydroxylamine),[26] which provides an avenue for (*E*)- and (*Z*)-nitrone interconversion.

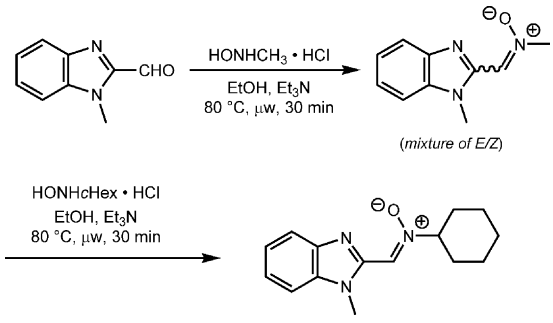

Scheme 4.

The Influence of R^1

Comparison of Entries 4, 7, 8, and 9 in Table 1 reveals the influence of R^1 on the relative amounts of products **A** and **B**. The experimental results demonstrate that as the size of R^1 gets larger (from H to Me to Ph, as R^2, R^3, and R^4 remain constant), the product distribution shifts steadily from a preponderance of **A** (see the discussion of R^3 below for an explanation for this inherent preference) to a preponderance of **B**. These cases are the ones for which our calculations of the transition-state energy deviate most (albeit slightly) from the experimental results. When R^1 = *t*Bu, no reaction occurs. Steric clashes involving R^1 are more significant for transition-state structures leading to product **A** (see Figure 3) – in transition structures leading to product **B**, R^1 points away from the rest of the molecule – selectively destabilizing this structure when R^1 is large, allowing product **B** to be produced preferentially.

The Influence of R^2

Comparison of Entries 4 and 11, where the only difference is the identity of R^2, shows that the size of R^2 has a dramatic effect on the relative proportions of products **A** and **B**. When R^2 is small (Entry 4), product **A** predominates (this is also true for Entries 1, 2, 3, 5 and 6), but when R^2 is large (Entry 11; see also Entry 12), only product **B** is observed. This effect is mirrored by the computed differences in transition-state-structure energies. Again, this appears to be a steric effect that selectively destabilizes transition-state structures leading to **A** (see Figure 3). When both R^1 and R^2 are larger than H, even when they are as small as methyl groups (Entries 13 and 14), product **B** again predominates.

The Influence of R^3

The importance of R^3 is revealed through a comparison of Entries 4, 15, 17, and 18 (where R^1, R^2, and R^4 remain constant). Formation of product **A** is inherently preferred

over formation of product **B** (e.g., see Entry 4, where R^3 = H). Increasing the size of R^3 (Entries 15, 17, and 18), however, leads to complete selectivity in favor of product **A**. This size effect is also manifested in the computed differences in transition-state-structure energies. As shown in Figure 3, R^3 is roughly eclipsed with a C–H bond at the other end of the forming C–C bond in transition-state structures leading to **B**, an unfavourable steric situation that is not present in transition-state structures leading to **A**.[27] In that the effects of having substituents at positions R^2 and R^3 on the cycloaddition selectivity are opposite, we decided to examine a system with substituents at both positions, here directly connected to each other – the cyclopentene shown in Scheme 5. For this system, the influence of neither position dominates, leading to a mixture of both cycloaddition products, in accord with the predicted difference of transition-state-structure energies of only 0.1 kcal/mol. These products were produced in low yield, however, with unreacted nitrone being formed as the major product.

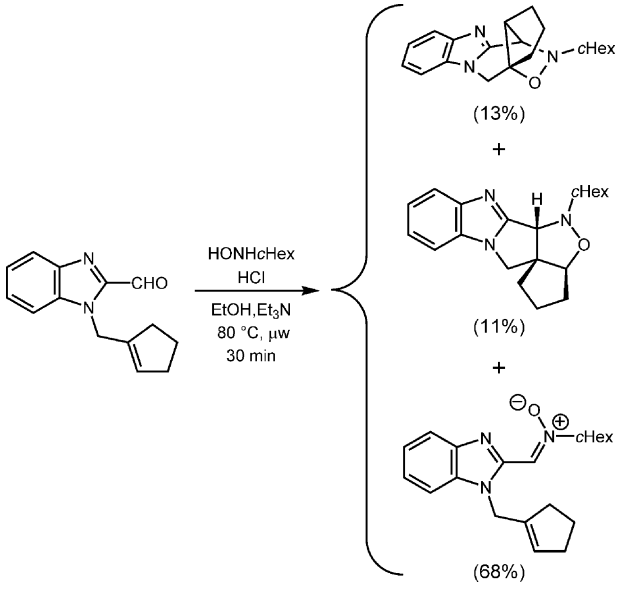

Scheme 5.

The Influence of R^4

As shown in Table 1, most of our experiments involved systems where R^4 = *c*Hex. We did, however, explore the influence of this group. In particular, the identity of R^4 was varied for systems where R^1 = R^2 = R^3 = H (Entries 1–6). The observed ratios of products **A** and **B** differed only slightly as R^4 was changed. As expected, when R^4 = H, no cycloaddition was observed and the oxime product was isolated instead (Scheme 6; see Supporting Information for details). This is clearly the result of *N*-deprotonation, which is not possible for the other systems.[28]

Several other comparisons were also made to see whether or not changing R^4 from *c*Hex affects the robustness of the selectivity for some of the most selective cases (e.g. Entries 11 vs. 12 and 13 vs. 14 for **A** and Entries 15 vs. 16 and 18 vs. 19 for **B**). These experiments show that the selectivity is affected only slightly by changing R^4, even for cases with substituents at R^1, R^2, or R^3.

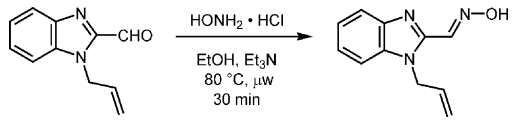

Scheme 6.

Conclusions

We have demonstrated the utility of microwave-assisted[31] intramolecular nitrone-alkene dipolar cycloadditions for the synthesis of two polyheterocyclic scaffolds that position their arrays of functional groups in well-defined but different orientations. A combination of experiment and theory was used to reveal general trends that can be used to control and predict the relative amounts of each type of product for these and closely related systems.[4] By changing the substituents on the dipolarophile, it is possible to achieve *complete* selectivity for *either* product: large substituents at position R^3 favor product **A** and large substituents at position R^2 favor product **B**.

Experimental Section

General: See ref.[7]

Representative Procedure for Cycloaddition: Reaction of 1-Allyl-1*H*-benzimidazole-2-carbaldehyde with *N*-Cyclohexylhydroxylamine (Entry 4): In a pyrex test tube, 1-allyl-1*H*-benzimidazole-2-carbaldehyde (74 mg, 0.4 mmol), triethylamine (0.06 mL, 0.44 mmol), and *N*-cyclohexylhydroxylamine hydrochloride (67 mg, 0.44 mmol) in absolute ethanol (5 mL) was submitted to microwave irradiation at 80 °C for 30 min. The solvent was removed under vacuum and the residue extracted with chloroform, washed with water and dried with sodium sulfate. After evaporation of the solvent, the resultant solid was purified by column chromatography on SiO_2 with the eluent of ethyl acetate and ethanol (100% to 90% ethyl acetate in gradient) to obtain two products. The first fraction gave product **B** and the second fraction contained product **A**.

(1*R,4*S**)-2-Cyclohexyl-1,2,4,5-tetrahydro-1,4-methano[1,2,5]oxadiazepino[5,4-*a*]benzimidazole (Entry 4, Product A):** Off-white solid (90 mg, 79%); m.p. 224–225 °C. IR (neat): $\tilde{\nu}_{max}$ = 3058, 2925, 2852, 1618, 1522, 1479, 1450, 1418, 1275, 1226, 1170, 776, 737 cm^{-1}. ^1H NMR (600 MHz, $CDCl_3$, 23 °C): δ = 7.740 (br. s, 1 H), 7.253 (br. s, 3 H), 4.903 (br. s, 1 H), 4.751 (br. s, 1 H), 4.138 (br. d, 1 H, *J* = 12 Hz), 3.950 (br. d, 1 H, *J* = 9.0 Hz), 2.889 (br. s, 1 H), 2.306 (br. d, 1 H, *J* = 8.4 Hz), 2.232 (br. s, 1 H), 1.105–2.000 (m, 10 H) ppm. ^{13}C NMR (150 MHz, $CDCl_3$, 23 °C): δ = 150.6, 143.0, 134.6, 123.1, 122.5, 120.2, 109.3, 71.1, 63.0, 55.7, 50.8, 36.2, 31.7, 30.3, 26.0, 24.6, 24.2 ppm. ESI MS: *m*/*z* = 284.12 $[M + H]^+$. Purity was determined to be 100% by HPLC analysis on the basis of absorportion at 214 nm.

(3a*R,10b*R**)-1-Cyclohexyl-1,3a,4,10b-tetrahydro-3*H*-isoxazolo-[3′,4′:3,4]pyrrolo[1,2-*a*]benzimidazole (Entry 4, Product B):** Off-white solid (22 mg, 19%); m.p. 200 °C (dec.). IR (neat): $\tilde{\nu}_{max}$ =

3053, 2934, 2856, 1620, 1526, 1487, 1456, 1420, 1329, 1220, 1177, 930, 764, 743 cm^{-1}; ^1H NMR (300 MHz, $CDCl_3$, 23 °C): δ = 7.730–7.771 (m, 1 H), 7.180–7.295 (m, 3 H), 4.903 (d, 1 H, J = 7.5 Hz), 4.127–4.224 (m, 2 H), 3.907–4.029 (m, 2 H), 3.838 (dd, 1 H, J = 9 Hz, 3 Hz), 2.820 (br. s, 1 H), 1.200–2.168 (m, 10 H) ppm. ^{13}C NMR (75 MHz, $CDCl_3$, 23 °C): δ = 158.1, 149.3, 132.1, 122.6, 122.4, 120.7, 110.0, 72.1, 63.4, 62.4, 49.8, 47.8, 31.6, 30.1, 26.1, 24.8, 24.7 ppm. ESI-MS: m/z = 284.12 $[M + H]^+$. Purity was determined to be 97% by HPLC analysis on the basis of absorportion at 214 nm.

Computations: GAUSSIAN03 was employed for all calculations.[32] All geometries were optimized at the B3LYP/6-31G(d) level of theory.[33] Structures for the system with $R^1 = R^2 = R^3 = H$, R^4 = Me were also optimized at the B3LYP/6-31+G(d,p) level of theory and no significant differences from the lower level of theory were observed (see Supporting Information for details). All stationary points were characterized as minima or transition structures by analyzing their vibrational frequencies (minima had only real frequencies and transition-state structures had one imaginary frequency). In select cases, intrinsic reaction coordinate (IRC) calculations were used to further characterize the identity of transition structures (see Supporting Information for details).[34] All reported energies include zero-point energy corrections from frequency calculations, scaled by 0.9806.[35] Transition-state energies in Table 1 are all relative to the lowest energy nitrone conformer found for a given system (see Supporting Information for structures). Due to the complexities associated with conformer distributions for nitrones, as well as the fact that these species are generated in situ experimentally, activation barriers are not discussed in detail in the text. Structures for the system with $R^1 = R^2 = R^3 = H$, R^4 = Me were also optimized at the CPCM(UAKS)-B3LYP/6-31+G(d,p)[36] level of theory to assess the effects of solvation (ethanol and chloroform were tested) and only minor differences from the gas-phase calculations were observed (see Supporting Information for details). Structural drawings in Figure 3 were produced using Ball & Stick.[37]

Supporting Information (see also the footnote on the first page of this article): Experimental details and characterization data for carbaldehydes, representative cycloadducts, nitrones, oximes, amides, and esters, as well as details on calculations, including full Gaussian citation, coordinates and energies.

CCDC-701193 (for Table 1, Entry 11, product **B**), -701194 (for Table 1, Entry 4, product **B**), -701195 (for Table 1, Entry 4, product **A**), -701196 (for compound **37** in Supporting Information), and -708168 (for Table 1, Entry 15, product **A**) contain the supplementary crystallographic data for this paper. These data can be obtained free of charge from The Cambridge Crystallographic Data Centre via www.ccdc.cam.ac.uk/data_request/cif.

Acknowledgments

We gratefully acknowledge the University of California, Davis and the National Science Foundation (NSF) (CAREER program, computer time from the Pittsburgh Supercomputer Center, and CHE-0614756), and the National Institutes of Health (NIH) (GM076151) for support of this work. NMR spectrometers used were partially funded by the NSF (CHE-0443516 and CHE-9808183).

[1] For leading references on intramolecular dipolar cycloadditions, see: a) I. Coldham, R. Hufton, *Chem. Rev.* **2005**, *105*, 2765–2810; b) V. Nair, T. D. Suja, *Tetrahedron* **2007**, *63*, 12247–12275; c) A. Padwa, S. K. Bur, *Tetrahedron* **2007**, *63*, 5341–5378; d) D. St. C. Black, R. F. Crozier, V. C. Davis, *Synthesis* **1975**, 205–221.

[2] R. R. K. Kumar, H. Mallesha, S. K. Rangappe, *Arch. Pharm. (Weinheim, Ger.)* **2003**, *336*, 159–164.

[3] B. G. Mullen, R. T. Decory, T. J. Mitchell, D. S. Allen, R. C. Kinsolving, *J. Med. Chem.* **1988**, *31*, 2008–2014.

[4] Closely related systems: a) with tether imidazole, $R^1 = R^2 = R^3 = H$, R^4 = Bn or phenylethyl: E. Beccalli, G. Broggini, A. Contini, I. De Marchi, G. Zecchi, C. Zoni, *Tetrahedron: Asymmetry* **2004**, *15*, 3181–3187 (gas phase MP2/6-311++G**//HF/6-31G** and MP2/6-31+G**//HF/6-31G** calculations were reported for two systems in this paper) and D. Basso, G. Broggini, D. Passarella, T. Pilati, A. Terraneo, G. Zecchi, *Tetrahedron* **2002**, *58*, 4445–4450 [consistent with our results (see Table 1), product **A** predominated for the two examples reported therein without additional allylic substituents]; b) with tether pyrrole or butylpyrrole, R^1 = H, Me, Pr, Ph, R^2 = H, Me, R^3 = H, R^4 = Bn, phenylethyl: G. Broggini, C. La Rosa, T. Pilati, A. Terraneo, G. Zecchi, *Tetrahedron* **2001**, *57*, 8323–8332; A. Arnone, G. Broggini, D. Passarella, A. Terraneo, G. Zecchi, *J. Org. Chem.* **1998**, *63*, 9279–9284 [consistent with our results (see Table 1), the six examples reported therein with R^2 and/or R^3 larger than H led to product **B** as the major product, while two of the three examples with $R^1 = R^2 = R^3 = H$ led to product **A** as the major product]; c) with tether indole, R^1 = Ph, R^2 = H, R^3 = H, R^4 = H, Bn, phenylethyl: E. M. Beccalli, G. Broggini, C. La Rosa, D. Passarella, T. Pilati, A. Terraneo, G. Zecchi, *J. Org. Chem.* **2000**, *65*, 8924–8932 [consistent with our results (see Table 1), for the two cases reported therein with $R^1 = R^2 = R^3 = H$, product **A** was the major product, and for the two cases with R^1 = Ph, product **B** was the major product]. Note that with a 3-methylindole tether, products of type **B** were reported for $R^1 = R^2 = R^3 = H$; see: D. St. C. Black, D. C. Craig, R. B. Deb-Das, N. Kumar, *Aust. J. Chem.* **1993**, *46*, 603–622; P. J. Bhuyan, R. C. Boruah, J. S. Sandhu, *Tetrahedron Lett.* **1989**, *30*, 1421–1422; d) For a system with a longer (aniline-derived) tether, see: G. Broggini, F. Colombo, I. De Marchi, S. Galli, M. Martinelli, G. Zecchi, *Tetrahedron: Asymmetry* **2007**, *18*, 1495–1501; e) For systems with cyclohexenes directly attached to the N of a pyrrole or indole tether, see: E. M. Beccalli, G. Broggini, A. Farina, L. Malpezzi, A. Terraneo, G. Zecchi, *Eur. J. Org. Chem.* **2002**, 2080–2086; in these cases, only products of type **B** were observed; f) For systems with inverted pyrrole tethers [i.e., CHR–C=$N^+(O^-)$Bn attached to N and a vinyl group attached to carbon], see: E. Borsini, G. Broggini, A. Contini, G. Zecchi, *Eur. J. Org. Chem.* **2008**, 2808–2816.

[5] M. A. Marx, A. L. Grillot, C. T. Louer, K. A. Beaver, P. A. Bartlett, *J. Am. Chem. Soc.* **1997**, *119*, 6153–6167.

[6] a) For our work on related cycloadditions using azomethine ylides, see: L. Meng, J. C. Fettinger, M. J. Kurth, *Org. Lett.* **2007**, *9*, 5055–5058; b) A 36 compound collection of the heterocycles reported in this manuscript has been added to the NIH Molecular Libraries Small Molecule Repository (MLSMR) for high-throughput biological screening.

[7] Experimental and computational details can be found in the Supporting Information.

[8] This is true even though the computed energies are for gas phase calculations. Tests on selected systems indicated that solvation (modeled using a continuum approach) has only small effects on the relative energies of the transition-state structures. See Supporting Information for details.

[9] M. Schelper, A. de Meijere, *Eur. J. Org. Chem.* **2005**, 582–592.

[10] T. Konoike, T. Hayashi, Y. Araki, *Tetrahedron: Asymmetry* **1994**, *5*, 1559–1566.

[11] C. Jimeno, M. Pasto, A. Riera, M. A. Pericas, *J. Org. Chem.* **2003**, *68*, 3130–3138.

[12] I. S. Kim, G. R. Dong, Y. H. Jung, *J. Org. Chem.* **2007**, *72*, 5424–5426.

[13] J. H. Rigby, S. V. Cuisiat, *J. Org. Chem.* **1993**, *58*, 6286–6291.
[14] W. G. Dauben, J. M. Cogen, G. A. Ganzer, V. Behar, *J. Am. Chem. Soc.* **1991**, *113*, 5817–5824.
[15] S. Yu, C. Rabalakos, W. D. Mitchell, W. D. Wulff, *Org. Lett.* **2005**, *7*, 367–369.
[16] D. D. Kim, S. J. Lee, P. Beak, *J. Org. Chem.* **2005**, *70*, 5376–5386.
[17] A. Chatterjee, D. K. Maiti, P. K. Bhattacharya, *Org. Lett.* **2003**, *5*, 3967–3969.
[18] I. Antonini, G. Cristalli, P. Franchetti, M. Grifantini, U. Gulini, S. Martelli, *J. Heterocycl. Chem.* **1978**, *15*, 1201–1203.
[19] A. Basak, S. C. Ghosh, *Tetrahedron Lett.* **2005**, *46*, 7385–7388.
[20] M. J. Haddadin, J. P. Freeman, *Chem. Heterocycl. Compd.* **1985**, *42*, 283–350.
[21] M. Lamchen, in *Mechanisms of Molecular Migrations* (Ed.: B. S. Thyagarajan), Interscience Publishers, New York, **1968**, vol. 1, pp. 1–60.
[22] Note also that no correlation was observed between the computed preference of a given nitrone for the *E* or *Z* geometry and the experimentally observed preference for a particular cycloaddition product. See Supporting Information for details on computed nitrone structures. Note also that for cases where nitrone products were observed (i.e., cycloaddition did not occur), mixtures of geometric isomers were observed when R^4 = Me but only one geometric isomer (of unknown stereochemistry) was observed when R^4 = *c*Hex.
[23] For a review, see: J. I. Seeman, *Chem. Rev.* **1983**, *83*, 83–134.
[24] a) Solvation single point calculations [CPCM(UAKS)-B3LYP/6-31G(d) using water] were also carried out, and these barriers do not change significantly. See Supporting Information for details; b) We are aware that the presence of the benzimidazole ring could significantly lower these barriers, but we have as yet been unable to locate analogous transition-state structures using larger models that include benzimidazole rings.
[25] a) Solvent induced shifts in the ^{1}H NMR spectra[25c] of these nitrones were used to make these *Z*/*E* assignments (data presented in the Supporting Information); b) Since *Z*/*E* assignment for this compound based on solvent induced shifts in the ^{1}H NMR spectra[25c] was ambiguous, this *Z* assignment is based on steric considerations[25c] (data presented in the Supporting Information); c) H. G. Aurich, M. Franzke, H. P. Kesselheim, *Tetrahedron* **1992**, *48*, 663–668.
[26] Note that reaction of the nitrone with 1-pentyne did not lead to any cycloadduct, consistent with the results described earlier for systems with tethered alkynes.
[27] This is an example of "torsional steering". For leading references, see: R. G. Iafe, K. N. Houk, *Org. Lett.* **2006**, *8*, 3469–3472.
[28] The pure oxime was subsequently heated in toluene under a nitrogen atmosphere in a sealed tube at 180 °C for 8 h,[29,30] but no desired cycloadduct was obtained.
[29] A. Hassner, R. Maurya, O. Friedman, H. E. Gottlieb, A. Padwa, D. Austin, *J. Org. Chem.* **1993**, *58*, 4539–4546.
[30] U. Chiacchio, G. Buemi, F. Casuscelli, A. Procopio, A. Rescifina, R. Romeo, *Tetrahedron* **1994**, *50*, 5503–5514.
[31] For leading references on microwave heating, see: a) C. O. Kappe, *Chem. Soc. Rev.* **2008**, *37*, 1127–1139; b) C. O. Kappe, D. Dallinger, *Nat. Rev. Drug Discovery* **2006**, *5*, 51–63; c) C. O. Kappe, *Angew. Chem. Int. Ed.* **2004**, *43*, 6250–6284.
[32] *Gaussian 03*, revision B.04, Gaussian, Inc., Pittsburgh, PA, **2004** (see Supporting Information for the full citation including all author names).
[33] a) A. D. Becke, *J. Chem. Phys.* **1993**, *98*, 5648–5652; b) A. D. Becke, *J. Chem. Phys.* **1993**, *98*, 1372–1377; c) C. Lee, W. Yang, R. G. Parr, *Phys. Rev. B: Solid State* **1988**, *37*, 785–789; d) P. J. Stephens, F. J. Devlin, C. F. Chabalowski, M. J. Frisch, *J. Phys. Chem.* **1994**, *98*, 11623–11627; e) The reliability of the B3LYP/6-31G(d) method for modeling dipolar cycloaddition reactions has been assessed previously. See, for example: D. H. Ess, K. N. Houk, *J. Phys. Chem. A* **2005**, *109*, 9542–9553; P. Merino, J. Revuelta, T. Tejero, U. Chiacchio, A. Rescifina, G. Romeo, *Tetrahedron* **2003**, *59*, 3581–3592.
[34] a) C. Gonzalez, H. B. Schlegel, *J. Phys. Chem.* **1990**, *94*, 5523–5527; b) K. Fukui, *Acc. Chem. Res.* **1981**, *14*, 363–368.
[35] A. P. Scott, L. Radom, *J. Phys. Chem.* **1996**, *100*, 16502–16513.
[36] a) V. Barone, M. J. Cossi, *J. Phys. Chem. A* **1998**, *102*, 1995–2001; b) B. Barone, M. Cossi, J. Tomasi, *J. Comput. Chem.* **1998**, *19*, 404–417; c) Y. Takano, K. N. Houk, *J. Chem. Theory Comput.* **2005**, *1*, 70–77.
[37] N. Müller, A. Falk, *Ball & Stick V.3.7.6*, molecular graphics application for MacOS computers, Johannes Kepler University, Linz, **2000**.

Received: December 4, 2008
Published Online: March 4, 2009

